Chaos, Solitons and Fractals 155 (2022) 111734

Contents lists available at ScienceDirect

Chaos, Solitons and Fractals

Nonlinear Science, and Nonequilibrium and Complex Phenomena

journal homepage: www.elsevier.com/locate/chaos

Frontiers

Dynamics of uncoupled and coupled neurons under an external pulsed current

Matheus Hansen[a], Paulo R. Protachevicz[b], Kelly C. Iarosz[c,d], Iberê L. Caldas[b], Antonio M. Batista[e,f,*], Elbert E.N. Macau[a]

[a] Institute of Science and Technology, Federal University of São Paulo - UNIFESP, São José dos Campos, São Paulo, SP, Brazil
[b] Institute of Physics, University of São Paulo, São Paulo, SP, Brazil
[c] Faculdade de Telêmaco Borba, FATEB, Telêmaco Borba, Paraná, Brazil
[d] Graduate Program in Chemical Engineering Federal Technological University of Paraná, Ponta Grossa, PR, Brazil
[e] Post-Graduation in Science, State University of Ponta Grossa, Ponta Grossa PR, Brazil
[f] Mathematics and Statistics Department, State University of Ponta Grossa, Ponta Grossa, PR, Brazil

ARTICLE INFO

Article history:
Received 7 September 2021
Revised 11 December 2021
Accepted 14 December 2021

Keywords:
Pulsed current
Hodgkin huxley neuron
Synchronisation

ABSTRACT

The neuron dynamics is highly susceptible to variations in its current input. In this work, we study the dynamics of uncoupled and random coupled Hodgkin Huxley neurons under an external current with constant or pulsed amplitude. The profile of these pulse perturbations are considered as periodic, random, and a mix between these two types. For uncoupled and coupled neurons submitted to a constant input current, we observe neuronal silence, spike, and coexistence between these two regimes, as well as spike synchronisation. However, when periodic pulse perturbations are introduced, the neuronal activities depend on the pulse parameters, as the amplitude and duration values. For random pulsed inputs, the complexity is greater, once such perturbation may induce the appearance of uncertainty in the neuronal dynamics. Furthermore, our simulations suggest that small time windows, in which the random pulses are embedded in a sequence of periodic pulses, are already enough to bring uncertainty in the neuronal activities. In such a scenario, the excitatory couplings can reduce these uncertainties around the behaviour developed by the neurons.

1. Introduction

In the human body, the brain is one of the most complex organ [1]. It is responsible for many different functions, such as motor [2], sensory [3], and cognition [4]. The brain is composed of billions of neurons [5] that transmit information through chemical and electrical synapses [6]. Researches in the neuroscience field aim to understand brain functions and how they are related to learning, memory, and many other cognitive functions.

Computational techniques and mathematical tools [7,8] have been used to analyse brain functions. Several types of mathematical models have been considered to mimic neuronal activities [9]. In the first decade of the 20th century, Lapicque [10] introduced a neuron model based on a simple capacitor circuit to compute neuronal firing frequency [11]. In 1952, Hodgkin and Huxley [12] proposed a neuron model that describes the action potential considering the ion channels. Various neuron models were inspired by the Hodgkin-Huxley model, such as the FitzHugh-Nagumo [13] and Morris-Lecar models [14].

Neuronal systems form complex networks of coupled neurons. A wide range of topologies has been utilised to model neuronal networks, for instance, random [15], small-world [16,17], and scale-free [18–20]. Antonopoulos et al. [21] studied the dynamical complexity in the C. elegans neuronal network [22,23]. In mammalian brains, the monkey and cat cortices were organised into networks with connected clusters of areas [24]. Recently, Coninck et al. [25] analysed the network properties of healthy and Alzheimer brains.

Networks of Hodgkin-Huxley (HH) neurons can mimic many neuronal phenomena that are observed in the brain. Borges et al. [26] demonstrated the effects of brain plasticity on the spiking activities by means of a network of coupled HH neurons. They showed that the neuronal behaviour depends on the network architecture and the external perturbation. Andreev et al. [27] found chimera states, namely the coexistence of different brain states, in networks of coupled bistable HH neurons. Depending on the system parameters and network topology, coupled HH neurons can

* Corresponding author.
E-mail address: abatista@uepg.br (A.M. Batista).

https://doi.org/10.1016/j.chaos.2021.111734
0960-0779/

exhibit synchronisation [28,29]. Wang et al. [30] reported that synchronisation can be supported by coherence resonance and noise in globally coupled HH neurons.

In this work, we focus on the study of the neuronal activities and identification of synchronous patterns in uncoupled and coupled excitatory HH neurons. These neurons are stimulated by an external current which has a constant or pulsed profile. Depending on the initial conditions, uncoupled neurons can exhibit different neuronal activities, such as silence, spike, and bistability (coexistence of these two regimes), as well as synchronised and desynchronised spike patterns for different amplitudes of the external current. Our numerical simulations suggest that the introduction of periodic pulses can produce relevant changes in the bistable ranges of the HH neurons, as well as in the ranges where the synchronous patterns are developed.

As reported by Nakamura and Tateno [31], a weak random pulse can induce phase synchronisation in uncoupled non-identical neuron models. We find that the application of random pulsed currents in the uncoupled neurons not only can support neuronal synchronisation, but also change the parameter range in which the bistability occurs. In such a case, if small amplitudes of the random pulses are considered, we verify an uncertainty involving the ranges in which the bistable activities or the spike synchronisation are developed. As uncertainty, we refer as the impossibility to predict the neuronal activity by a small variation of the parameter value. Due to this fact, there are some neighbourhood values in the parameter space such that the initial conditions generate different dynamic behaviours.

For coupled HH neurons, we study the emergence of different neuronal activities and the onset of synchronous behaviour. In the absence of pulses, the synchronisation arises through the increase of the coupling strength among the HH neurons. For weak coupling strength, we verify that the pulsed currents can change the parameter range in which the bistable activities appear and also support spike synchronisation.

The main goal of our work is to investigate how synchronisation and bistability emerge in a neuronal network due to different current pulsed protocols. There is a great interest in studying the effects of external perturbations on neuronal network dynamics. Protachevicz et al. [32] demonstrated that external stimulation not only can induce neuronal synchronisation, but also can reduce abnormal synchronous behaviour. This way, epileptic seizures may be controlled or treated. Recently, Cota et al. [33] applied an electrical stimulation in rats submitted to pentylenetetrazole-induced acute seizures. They reported that experimental nonperiodic stimulation can be a promising alternative for the treatment of epilepsy. Considering a model similar to the one introduced in [33], one of our main results suggests that nonperiodic stimulation, according to a random protocol, can generate uncertainties in the neuronal activities and synchronisation. The appearance of uncertainties is a theoretical advance in the studies related to brain disorders.

This paper is organised as follows. In Section II, we introduce the neuron model and the neuronal network. In Section III and IV, we discuss our results about neuronal synchronisation in uncoupled and coupled neurons under external pulsed currents, respectively. In the last section, we present our conclusions.

2. Neuronal network

The HH neuron is one of the most important and famous models in computational neuroscience. This model was proposed in 1952 by Hodgkin and Huxley [12] in order to describe the generation mechanisms of the action potential in experiments with the squid giant axon. In their work, it was reported that the generation of the action potential in the cell membrane is related to the variations in the ionic currents of potassium (K), sodium (Na), and a current defined by them as leak (l). The HH model is given by

$$C\frac{dV_i}{dt} = -g_{\rm K}n_i^4(V_i - V_{\rm K}) - g_{\rm Na}m_i^3h_i(V_i - V_{\rm Na}) - g_{\rm l}(V_i - V_{\rm l}) + I^{\rm ext} + I_i^{\rm syn}, \tag{1}$$

$$\frac{dx_i}{dt} = \alpha_{x_i}(v_i)(1 - x_i) - \beta_{x_i}(v_i)x_i, \tag{2}$$

$$\frac{ds_i}{dt} = \frac{5(1 - s_i)}{1 + \exp\left(\frac{-v_i+3}{8}\right)} - s_i, \tag{3}$$

where C is the capacitance of the cell membrane and V_i is the membrane potential for the i-th neuron. The variables n_i and m_i are related to the potassium (K) and sodium (Na) channel activations, respectively, while h_i is associated with the sodium (Na) channel inactivation. In Eq. (2), $x_i = n_i, m_i, h_i$ and $v_i = V_i/[\text{mV}]$ is the dimensionless membrane potential. α_{x_i} and β_{x_i} are experimental functions written as

$$\alpha_n(v_i) = \frac{0.01v_i + 0.55}{1 - \exp(-0.1v_i - 5.5)}, \tag{4}$$

$$\alpha_m(v_i) = \frac{0.1v_i + 4}{1 - \exp(-0.1v_i - 4)}, \tag{5}$$

$$\alpha_h(v_i) = 0.07\exp\left(\frac{-v_i - 65}{20}\right), \tag{6}$$

$$\beta_n(v_i) = 0.125\exp\left(\frac{-v_i - 65}{80}\right), \tag{7}$$

$$\beta_m(v_i) = 4\exp\left(\frac{-v_i - 65}{18}\right), \tag{8}$$

$$\beta_h(v_i) = \frac{1}{1 + \exp(-0.1v_i - 3.5)}. \tag{9}$$

Equation (3) describes the temporal variation of the post-synaptic potential s_i of the neuron i [34,35].

We consider that the HH neurons are stimulated over time by the same external current $I^{\rm ext}$, which is defined as

$$I^{\rm ext} = I_0 + \Theta(t), \tag{10}$$

where I_0 corresponds to a current with constant amplitude (in μA/cm^2) and $\Theta(t)$ represents the pulses with amplitude Γ, that can be added to I_0 during a time considering some conditions. In our simulations, if $\Theta(t)$ assumes a value equal to zero for all times, the external current is equal to I_0, configuring an external current with constant amplitude. However, if the external current is pulsed, $\Theta(t)$ assumes a value equal to 0 or Γ in an on-off configuration along time. In this work, we consider a constant and three pulsed current profiles applied in the neurons. Figs. 1(a), 1(b), 1(c), and 1(d) display a schematic representation of external currents. The first case (Fig. 1(a)) is a constant current, while the second one is a periodic pulsed current (Fig. 1(b)), in which the on-off transition in $\Theta(t)$ during the simulation occurs in equal and fixed time interval Δt. Fig. 1(c) shows a pulse in which the transition on-off in $\Theta(t)$ has time intervals Δt randomly distributed (random uniform distribution). In Fig. 1(d), we define a time window $\lambda_{\rm P}$ and $\lambda_{\rm R}$ (in ms) in which the external current assumes sequentially periodic and random pulses along time, respectively. The pulses studied in this work can be related to different sensory stimulus that arrive in the HH neurons over time [31,33].

We consider that the HH neurons are excitatory and the interaction among them is by means of chemical synapses. We only consider excitatory due to the fact that they are the predominant type found in the nervous system. According to Noback et al.

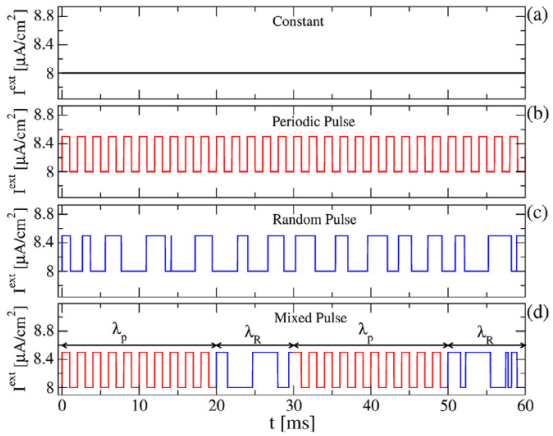

Fig. 1. Schematic representation of external currents: (a) constant amplitude $I_0 = 8$ μA/cm^2, (b) periodic pulses for $I_0 = 8$ μA/cm^2, $\Delta t = 1$ ms, and $\Gamma = 0.5$ μA/cm^2, (c) random pulses for $I_0 = 8$ μA/cm^2 with $\Gamma = 0.5$ μA/cm^2, and (d) mixed pulses with time windows $\lambda_P = 20$ ms and $\lambda_R = 10$ ms.

[36], approximately 80% are excitatory and 20% are inhibitory. The synaptic currents are given by

$$I_i^{syn} = (V_r^{exc} - V_i)\frac{g_{exc}}{N_i}\sum_{k=1}^{N} A_{ik}s_k, \tag{11}$$

where V_r^{exc} is the excitatory reversal potential, N is the number of the neurons, and N_i is the number of excitatory pre-synaptic connections of each neuron i given by the adjacency matrix A_{ik}. The g_{exc} (mS/cm^2) parameter is the excitatory synaptic conductance from the pre-synaptic neuron k to the post-synaptic neuron i.

Following [26], we consider $N = 100$ neurons that are randomly coupled (random uniform distribution) with a probability of connections $p = .1$. The initial conditions are randomly distributed in $V_i \in [-60, -40]$ mV, while $n_i = m_i = h_i = s_i = 0$. In our simulations, we use the fourth-order Runge-Kutta algorithm with a fixed integration time step $\delta t = 10^{-2}$ ms. Table 1 exhibits the description and values of the parameters [26,27,38], as well as the units and ranges.

Table 1
Description of the parameters, values, units, and ranges used in our numerical simulations of the uncoupled and coupled HH neurons [26,37,38].

Description	Parameter	Values
Number of neurons	N	100
Connection probability	p	0.1
Excitatory synaptic conductance	g_{exc}	[0,0.01] mS/cm^2
Membrane capacity	C	1.0 μF/cm^2
Potassium conductance	g_K	36 mS/cm^2
Sodium conductance	g_{Na}	120 mS/cm^2
Leak conductance	g_l	0.3 mS/cm^2
Potassium reversal potential	V_K	-77 mV
Sodium reversal potential	V_{Na}	50 mV
Leak reversal potential	V_l	-54.4 mV
Excitatory reversal potential	V_r^{exc}	20 mV
Constant current	I_0	[8,15] μA/cm^2
On-off pulse amplitude	Γ	[0,4]μA/cm^2
On-off time interval	Δt	[0,10] ms
Time step integration	δt	10^{-2} ms
Initial time for analyses	t_{ini}	1 s
Final time for analyses	t_{fin}	2 s
Initial window of periodic pulses	λ_P^0	200 ms
Time window of periodic pulses	λ_P	[0,200] ms
Time window of random pulses	λ_R	[0,200] ms

3. Uncoupled neurons

3.1. External current with constant amplitude

As reported in the literature, the behaviour of the HH neuron is separated into two different states [26,27]. The first state is the spike, which is characterised by a sudden increase in the membrane potential value. The second state is the silent, in which the membrane potential exhibits a small oscillation amplitude around the resting potential. These patterns are displayed in the inset box of Fig. 2(a), where the blue and red lines are the spike and silent behaviours, respectively. The spike state is reached when the solution of the system converges to a limit cycle (LC), while the silent state occurs due to convergence to the fixed point (FP). The transition from one state to another is related to a Hopf bifurcation in the system [39]. Depending on the initial conditions, the value of I_0 can be or not enough to lead the neurons from the silent to spike states. Through the variation of I_0, it is possible to find patterns in which all neurons are in silence, spiking or even in a merged form between both states, where a fraction of neurons spikes and an-

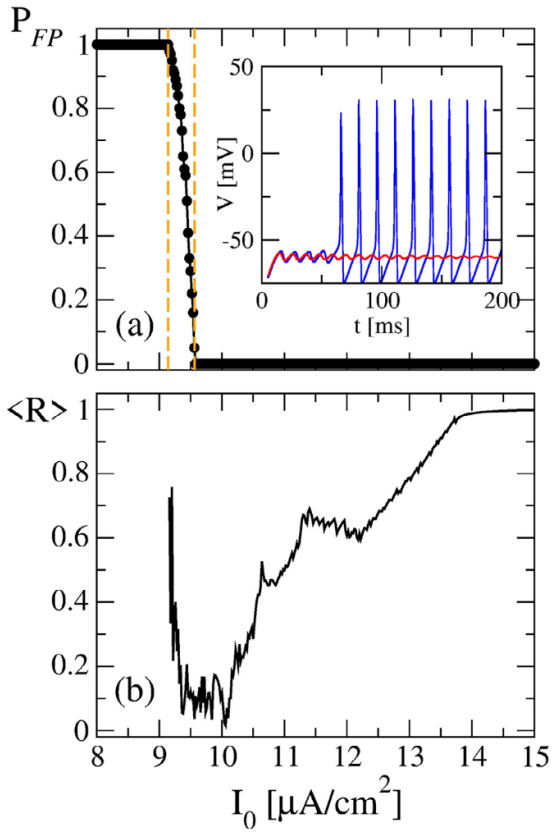

Fig. 2. (a) Fixed point probability P_{FP} as a function of a current with constant amplitude I_0 applied in the uncoupled HH neurons. All neurons are in silence for $P_{FP} = 1$, while they are in spike activities for $P_{FP} = 0$. The transition from $P_{FP} = 1$ to $P_{FP} = 0$ represents the range of I_0 in which a fraction of the neurons can be in spike activities and another in silence, due to the bistability behaviour. The inset box exhibits the states of silence (red line) and spike (blue line). (b) Mean order parameter $\langle R \rangle$ as a function of I_0. We observe that the neurons can be all in inactive or active states, as well as in a bistable activity. For a constant current, it is possible to identify synchronous and desynchronous states. In our simulations, we consider 100 neurons. (For interpretation of the references to colour in this figure legend, the reader is referred to the web version of this article.)

other remains in silence due to the bistability. In the inset box of Fig. 2(a), we show an example of bistable activity for two uncoupled HH neurons with different initial conditions and submitted to the same currents with constant amplitude $I_0 = 9.26\ \mu A/cm^2$.

In order to estimate the range of I_0 in which the bistability appears, we analyse the behaviour of the fixed point probability P_{FP}. This diagnostic tool indicates the fraction of neurons that reach the fixed point according to the I_0 value. Considering $t = 2$ s, as shown in Fig. 2(a), the values of P_{FP} equal to 1 and 0 correspond to the behaviours in which all neurons are in the fixed point (silence) and limit cycle (spike), respectively. For a current with constant amplitude, the bistability occurs in the interval $9.14\ \mu A/cm^2 < I_0 < 9.56\ \mu A/cm^2$ (between the orange dashed lines).

Aiming to study neuronal synchronisation, we calculate the mean value of the Kuramoto order parameter [40]

$$\langle R\rangle = \frac{1}{t_{\rm fin}-t_{\rm ini}}\int_{t_{\rm ini}}^{t_{\rm fin}}\left|\frac{1}{N_{\rm spike}}\sum_{i=1}^{N_{\rm spike}}\exp[{\rm j}\Phi_i(t)]\right|dt, \tag{12}$$

where $t_{\rm ini} = 1$ s and $t_{\rm fin} = 2$ s corresponds to the initial and final times of the analyses, $N_{\rm spike}$ is the number of spiking neurons (in the limit cycle), and j is an imaginary number defined as ${\rm j} = \sqrt{-1}$. The phase $\Phi_i(t)$ is given by

$$\Phi_i(t) = 2\pi m + 2\pi\frac{t - t_{i,m}}{t_{i,m+1} - t_{i,m}}, \tag{13}$$

where $t_{i,m}$ is the time at the m-th spike from neuron i occurs. The mean order parameter $\langle R\rangle$ belongs to a range from 0 to 1, where the synchronisation is identified when $\langle R\rangle \approx 1$.

Fig. 2 (b) shows $\langle R\rangle$ as a function of I_0. Increasing I_0, we see that $\langle R\rangle$ increase after the bistability range. For $I_0 \geq 13.5\ \mu A/cm^2$, I_0 induces the same activity to all uncoupled neurons ($g_{\rm exc} = 0$ mS/cm^2).

Fig. 3 (a) shows the raster plot for $I_0 = 9.4\ \mu A/cm^2$. We observe the coexistence of neurons in silence and spiking states. In Figs. 3(b) and 3(c), the raster plots indicate that for $I_0 = 9.75\ \mu A/cm^2$, which corresponds to a small amplitude current, the neurons exhibit desynchronised spikes ($\langle R\rangle \approx 0.1$) over time, while for $I_0 = 13.5\ \mu A/cm^2$, they have their spike activities synchronised ($\langle R\rangle \approx 0.9$). Therefore, depending on the current amplitude, different spike regimes can be generated.

In this subsection, our main result is the appearance of synchronous behaviour, in uncoupled neurons, considering that the initial conditions are randomly distributed with a small variance.

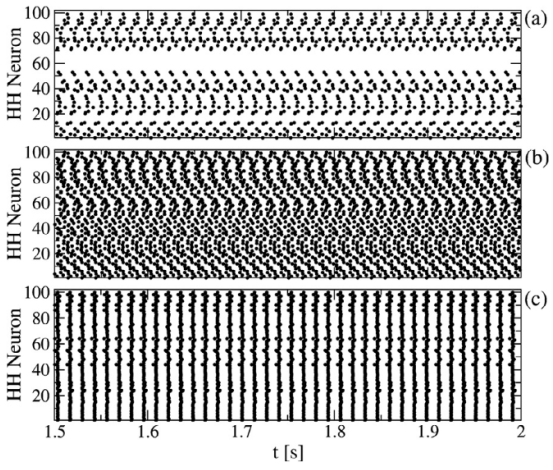

Fig. 3. Raster plots for (a) $I_0 = 9.4\ \mu A/cm^2$ (coexistence of neurons in silence and spiking states), (b) $I_0 = 9.75\ \mu A/cm^2$ (desynchronous behaviour $\langle R\rangle \approx 0.1$) and (c) $I_0 = 13.5\ \mu A/cm0^2$ (synchronous behaviour $\langle R\rangle \approx 0.9$).

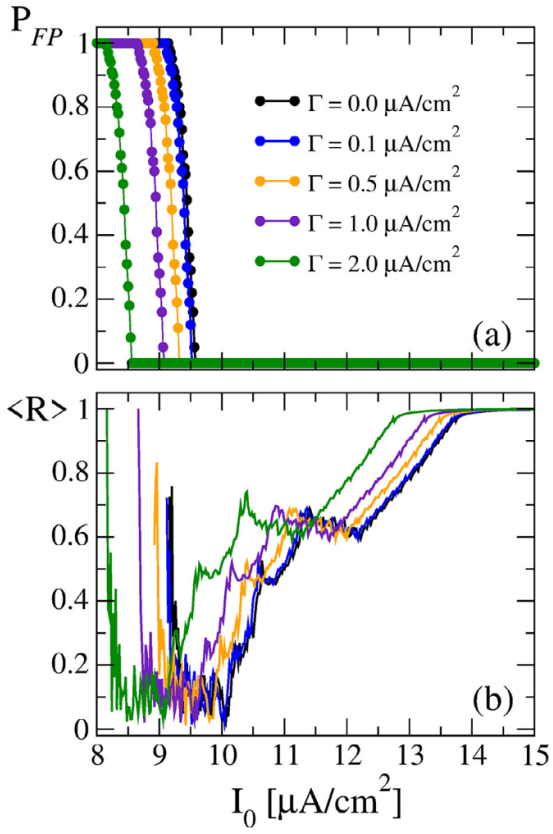

Fig. 4. (a) P_{FP} as function of I_0 with $\Delta t = 1$ ms for different values of Γ. The perturbation changes the range of I_0 in which the bistable activity (transition from $P_{FP} = 1$ to $P_{FP} = 0$) appears. (b) $\langle R\rangle$ as a function of I_0. Increasing Γ, the pulses can anticipate the beginning of the spike synchronisation. We observe that pulsed currents change the bistability and synchronous curve. The regions of bistability are anticipated. In our simulations, we consider 100 HH neurons.

For small I_0 values, a vast majority of neurons remains in a silence state (fixed point). Increasing I_0 and depending on the initial conditions, the solution of the neuron model can go to a limit cycle (spike state). For high I_0 values, most of solutions go to a limit cycle almost at the same time, and as a consequence of this fact, it is possible to observe synchronous behaviour.

3.2. External current with periodic pulses

Perturbations applied in neurons have important meanings in the context of neuronal dynamics, due to the fact that perturbations can be associated with stimulus on the sensory perceptions, promoting changes in the individual or collective behaviour of the neurons. With this in mind, we introduce pulsed perturbations in the neuronal model, as indicated in Eq. (10), where $\Theta(t)$ represents a pulse that assumes a value equal to 0 and Γ in an on-off configuration for equal and fixed time intervals Δt (Fig. 1(b)).

Fig. 4 displays our results for $\Delta t = 1$ ms and different values of Γ. As shown in Fig. 4(a), the pulses play a relevant role in the changes of the activities developed by the uncoupled neurons. The increase of Γ produces anticipation in the range of I_0 related to the bistability. The synchronised spikes appear for smaller values of I_0 when the Γ amplitude is increased, as shown in Fig. 4(b).

The pulses change not only the neuronal activity from silence (FP) to spiking behaviour (LC), but also the bistable range, due to the fact that the perturbations promote small changes along the orbit of the HH neurons. In some cases, small changes are enough

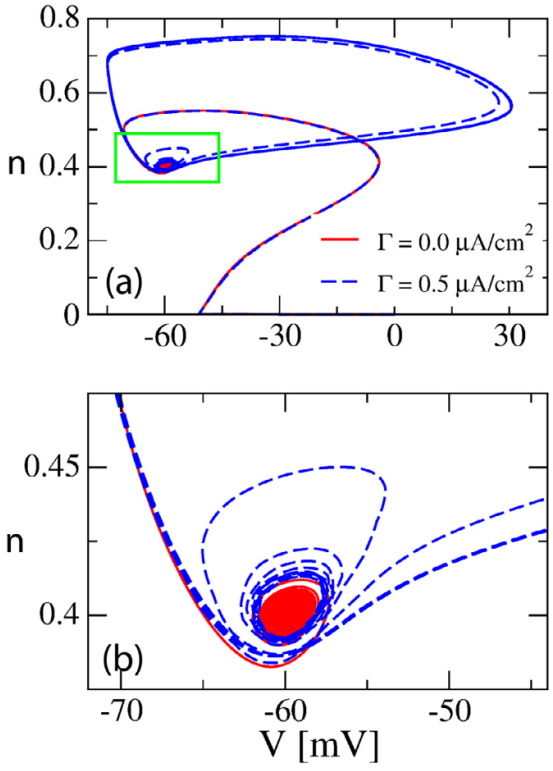

Fig. 5. (a) Phase space $n \times V$ and (b) magnification for one HH neuron, where the red and blue lines represent the orbits which converge to a fixed point (silence state) without perturbation and to a limit cycle (spike state) with perturbation, respectively. For the perturbed case, we consider $\Gamma = 0.5$ μA/cm^2 and $\Delta t = 1$ ms. The blue and red lines correspond to the active and inactive states, respectively. In our simulations, we consider 100 HH neurons. (For interpretation of the references to colour in this figure legend, the reader is referred to the web version of this article.)

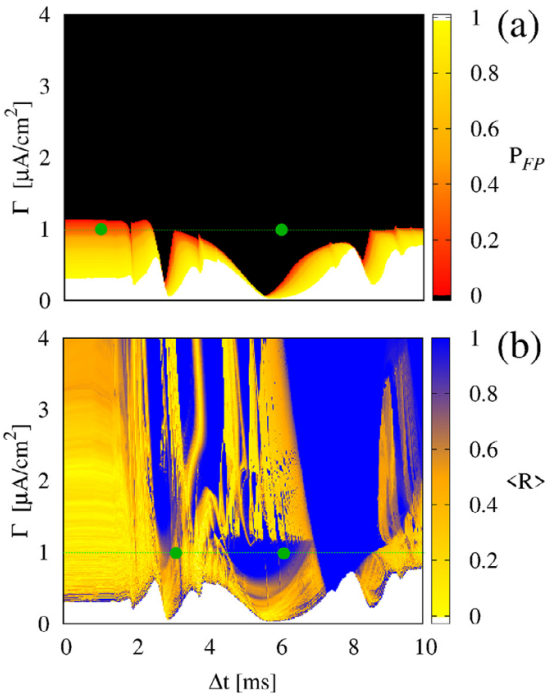

Fig. 6. Parameter space $\Gamma \times \Delta t$ for uncoupled neurons under an external current periodically pulsed. We consider $I_0 = 9.0$ μA/cm^2, which in the absence of perturbation configure a situation where all HH neurons are in silence (fixed point). The panel (a) displays P_{FP} in colour scale (1 and 0 means that all neurons are in silence and spike activities, respectively). For Δt equal to 1 ms and 6 ms, we observe bistability and spike activities, respectively (green dots). The panel (b) shows the mean order parameter $\langle R \rangle$ in the colour scale. For Δt equal to 3 ms and 6 ms, we observe desynchronous and synchronous spike patterns, respectively (green dots). The bistable region can be changed due to the periodic pulses and depends on Δt and Γ. The synchronous behaviour depends on Γ and Δt. In our simulations, we consider 100 HH neurons. (For interpretation of the references to colour in this figure legend, the reader is referred to the web version of this article.)

to switches the basin of attraction, altering the neuronal activities. A representation of the action of a perturbation in the neuronal dynamics is displayed in Fig. 5(a) through the phase space $n \times V$. In the absence of pulses, the orbit converges to the fixed point (red line). However, when a small periodic perturbation with $\Gamma = 0.5 \mu$A/cm^2 and $\Delta t = 1$ ms is applied, the orbit (blue line) goes to a limit cycle. Fig. 5(b) exhibits a magnification of the phase space of Fig. 5(a) indicated by a green rectangle.

We analyse the emergence of spikes and silence states, as well as synchronous and desynchronous states by means of the parameter space $\Gamma \times \Delta t$, considering the time interval $\Delta t \in [0, 10]$ ms and $\Gamma \in [0, 4] \mu$A/cm^2. The range of $2\Delta t$ corresponds to a cycle of the perturbation (on-off). In this way, the frequencies produced by the perturbation are comparable to the mean spike frequency of the HH neurons, about 71 Hz ($\Delta t \sim 7$ ms) [26], superiors ($\Delta t < 7$ ms) and lowers too ($\Delta t > 7$ ms). In Figs. 6(a) and 6(b), we compute $\Gamma \times \Delta t$ for $I_0 = 9$ μA/cm^2, where the colour bars correspond to P_{FP} and $\langle R \rangle$, respectively. Our results show that Δt and Γ play an important role in the bistability range and also in the emergence of synchronous patterns. We observe that for $\Gamma = 1$ μA/cm^2, the bistable behaviour occurs for $\Delta t = 1$ ms (500 Hz). $0 < P_{FP} < 1$ in the bistable behaviour. However, for $\Delta t = 6$ ms (83 Hz), the same Γ value is enough to lead all neurons to exhibit spikes (green dots in Fig. 6(a)). The change happens only by varying the time interval in which the pulse is on-off. For $\Gamma = 1$ μA/cm^2, it is possible to see in Fig. 6(b) (green dots) desynchronous and synchronous spikes patterns for $\Delta t = 3$ ms (167 Hz) and $\Delta t = 6$ ms (83 Hz), respectively. Our numerical simulations show that the periodic pulses in the external current can affect the dynamics of a single HH neuron, as well as the collective dynamics developed by them, mainly in the context of the emergence of spike activities and synchronisation.

3.3. External current with random pulses

We consider pulses with Δt randomly distributed (random uniform distribution) in the interval [0,10] ms (Fig. 1(c)). In order to discuss the effects of random pulses in the neurons, we analyse the parameter space $\Gamma \times I_0$ computing P_{FP} and $\langle R \rangle$. Figure 7(a) displays the emergence of neuronal spiking. Increasing Γ, the random pulses can change the range in which the bistable activity appears. Differently from the periodic pulses, where the ranges in which the appearance of the bistability is well defined, the random pulses tend to develop a type of uncertainty about the ranges where these activities are exhibited, as shown in Fig. 7(a). In order to highlight the uncertainty behaviour, we show in Fig. 7(b) a magnification of the parameter space $\Gamma \times I_0$ (green box in Fig. 7(a)). Due to the uncertainty, it is not possible to define the ranges where the bistable states appear.

With regard to the spike synchronisation, our results indicate that the random pulses can support synchronisation in the uncoupled HH neurons for $\Gamma > 2 \mu$A/cm^2, as shown in Fig. 7(c). In this range, we observe just few points related to desynchronised states. On the other hand, we find uncertainties associated with the synchronous and desynchronous patterns for $\Gamma < 2$ μA/cm^2. The uncertainties are well highlighted in Fig. 7(d) (green box in Fig. 7(c)).

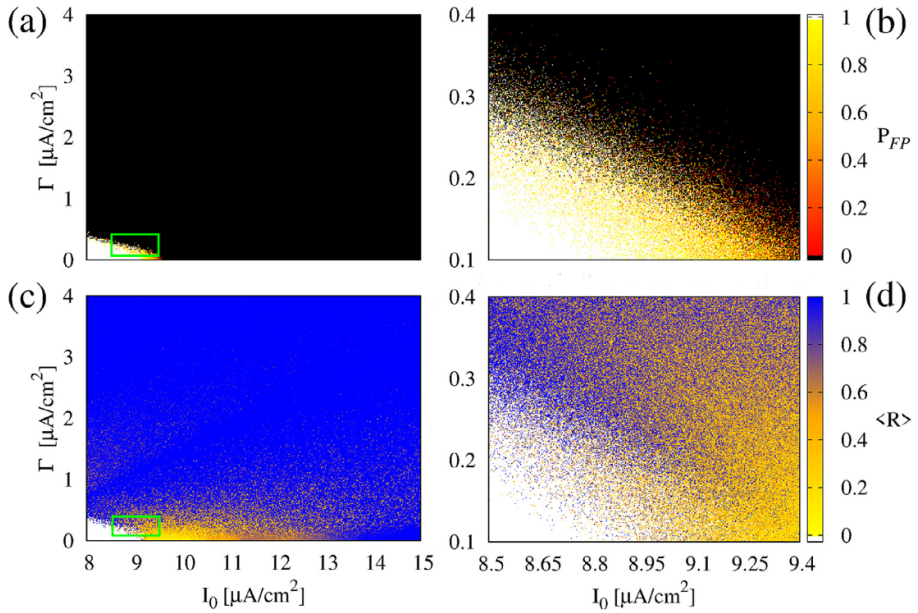

Fig. 7. Parameter space $\Gamma \times I_0$ for uncoupled HH neurons under a random pulse. The panels (a) and (b) display the P_{FP} in colour scale. The panels (c) and (d) show the mean order parameter $\langle R \rangle$ in colour scale. The random pulses induce uncertainties close to the transition and bistable regions, as well as in the synchronisation for the parameters in which the neurons are active. In our simulations, we consider 100 HH neurons.

3.4. External current with mixed pulses

Chatterjee and Robert [41] reported that introducing some amount of noise into stimulus may improve auditory perception in chochlear implants. They considered random fluctuations uniformly distributed within a specified range. We study the case in which the external current applied on the neurons is composed of periodic and random pulses, leading to a mixed pulse profile. We separate the external current into windows λ_P and λ_R (in ms), as illustrated in Fig. 1(d). In our simulations, we define the relation about the sizes of these windows as

$$\lambda_P = \lambda_P^0 - \lambda_R, \tag{14}$$

where $\lambda_P^0 = 200$ ms represents the size of an initial window of periodic pulses, while λ_R is the size of the window for the random ones. For $\lambda_R = 0$, the external current is a periodic pulse. On the other hand, if $\lambda_R > 0$ ms, the external current is composed of sequences of periodic and random pulses (Fig. 1(d)). If $\lambda_R = \lambda_P^0$, there are no windows of periodic pulses and the external current is a random pulse.

We analyse the effects of windows with different sizes of random and periodic pulses on the neuronal activities. To do that, we initially select a periodic pulse profile with $I_0 = 9.0$ μA/cm^2 and $\Delta t = 1$ ms, and then we calculate P_{FP} and $\langle R \rangle$ varying Γ and λ_R, as shown in Fig. 8(a) (green box in Fig. 8(b)). As λ_R increases, there is a reduction of the region where no spikes are fired.

Regarding the spike synchronisation, Fig. 8(c) (green box in Fig. 8(d)) displays that small windows of random pulses are enough to induce uncertainty about the neuronal activities. Our results suggest that small variations in the profiles of some sensory stimulus can change significantly the dynamics of the neurons, which in some cases can be undesirable, mainly in the context of neurological disorders.

4. Coupled neurons

In this section, we study the effects of different profiles of external currents applied in a network of coupled HH neurons. The neurons are randomly coupled by means of chemical synapses. In our simulations, we repeat the same procedures developed along the section before. Initially, we analyse the parameter space $g_{exc} \times I_0$ for the scenario in which the external current has a constant amplitude. As displayed in Fig. 9(a), the coupling strength g_{exc} can be enough to modify some neuronal activities of the network. One of these modifications is verified looking to the range of I_0 in which the bistability occurs. In this range, it is possible to find chimera state, which is the coexistence of neurons in silence and spiking states [27]. As indicated by the green dashed line, as g_{exc} increases, the bistable activity of the neuronal network ($0 < P_{FP} < 1$) is reduced, and the emergence of the total spike activities ($P_{FP} = 0$) is anticipated. Fig. 9(b) shows that for $g_{exc} > 0.015$ mS/cm^2 (and after the bistable region, $I_0 \gtrapprox 9.25$) synchronisation is achieved. On the other hand, for 0 mS/cm^2 $< g_{exc} <$ 0.015 mS/cm^2, the spike synchronisation can be reached by increasing I_0, indicating a possibility of spike synchronisation in neurons weakly coupled by adjusting the amplitude of the external stimulus. We consider that the coupling is weak for $g_{exc} \lessapprox 0.015$ mS/cm^2.

Aiming to find synchronisation in a network with neurons weakly coupled and under an external current, we consider periodic pulses with $\Gamma = 0.35 \mu$A/cm^2 and $I_0 = 9.0$ μA/cm^2. Figs. 10(a) and 10(b) exhibit the parameter space $g_{exc} \times \Delta t$ with P_{FP} and $\langle R \rangle$ in colour scales, respectively. The periodic pulse, even with small amplitude, applied in specific time intervals Δt is enough to anticipate the bistable range and promotes the emergence of neuronal neuronal spiking. The presence of pulses can also favour the appearance of spike synchronisation for small couplings strength, for instance in the case where $\Delta t \approx 6$ ms.

For random pulses with $\Gamma = 0.35$ μA/cm^2, we verify that the bistability appears for smaller values of I_0 when compared with the case of the absence of pulses (Fig. 9(a)), as shown in Fig. 11(a). However, we found that the parameter range, in which the bistability occurs, is composed of straight lines along the parameter space, where P_{FP} intermittently changes its value. This pattern is also observed in the magnification shown in Fig. 11(b) (green box in Fig. 11(a)). It is important to observe that this effect is correlated with the uncertainty verified in the case of the uncoupled neurons.

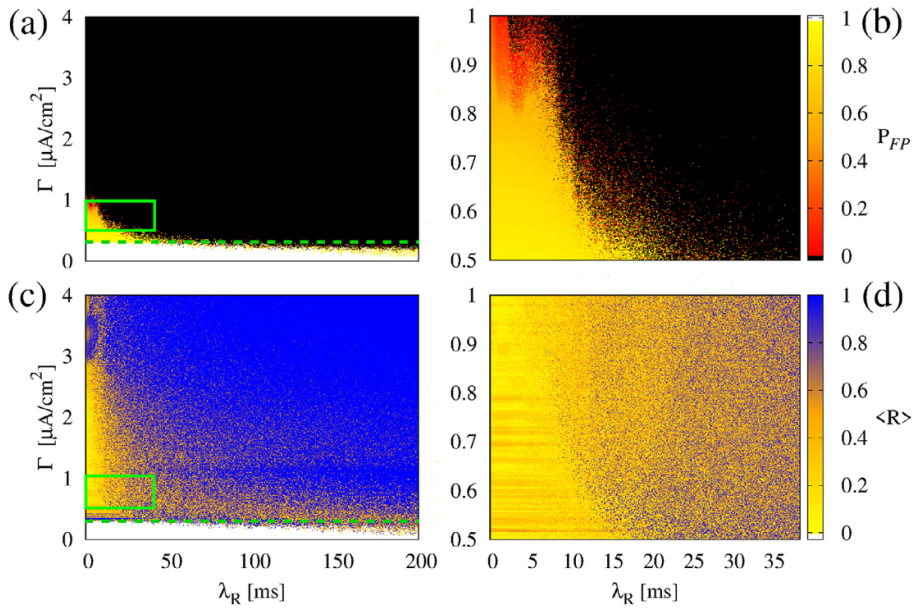

Fig. 8. Parameter space $\Gamma \times \lambda_R$ for uncoupled HH neurons under an external current with mixed pulses considering $I_0 = 9$ μA/cm^2. The panels (a) and (b) display the P_{FP} in colour scale. The panels (c) and (d) show the mean order parameter $\langle R \rangle$ in colour scale. We verify that small time windows of random pulses can generate uncertainties in the active or inactive states and synchronisation. In our simulations, we consider 100 HH neurons.

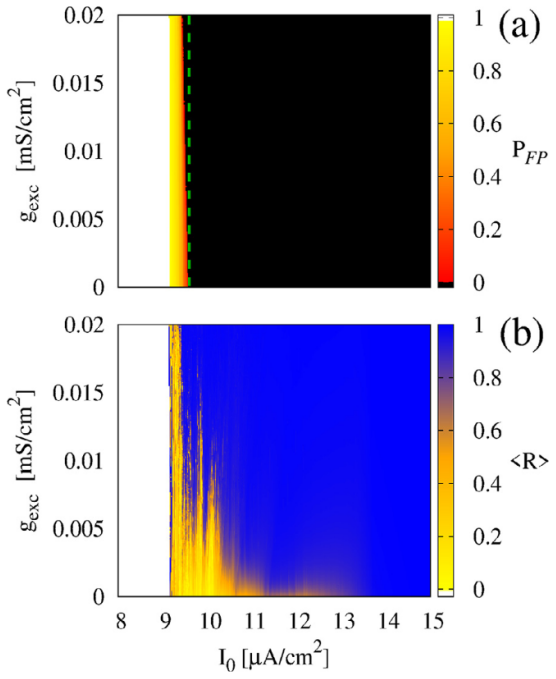

Fig. 9. Parameter space $g_{exc} \times I_0$ for coupled HH neurons under an external constant current of amplitude I_0. The panel (a) displays P_{FP} in colour scale. The panel (b) shows the mean order parameter $\langle R \rangle$ in colour scale. The increase of the coupling can reduce the size of the bistable region and promote the emergence of synchronisation.

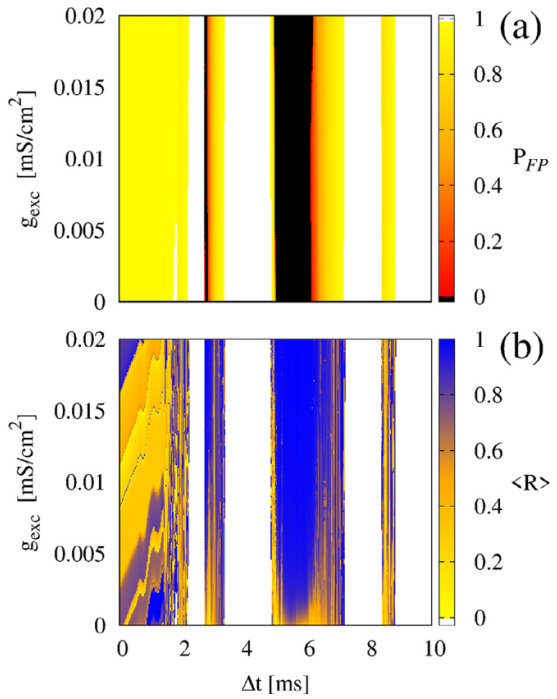

Fig. 10. Parameter space $g_{exc} \times \Delta t$ for coupled HH neurons under an external current periodically pulsed with $I_0 = 9.0$ μA/cm^2 and $\Gamma = 0.35$ μA/cm^2. The panel (a) displays P_{FP} in colour scale. The panel (b) shows the mean order parameter $\langle R \rangle$ in colour scale. The synchronous behaviour depends not only on the coupling strength, but also on Δt.

When the neurons are uncoupled, the uncertainty is found through a complex mix of dots along the parameter space (Fig. 7(a) and 7(b)), while in the coupled scenario (Fig. 11(a) and 11(b)), it manifests via this thin merged straight lines along $g_{exc} \times I_0$.

Concerning the synchronisation of spike activities, the uncertainty can also appear due to the random pulses. Fig. 11(c) displays thin lines that indicate synchronous and desynchronous states. Fig. 11(d) (green box in Fig. 11(c)) also shows thin lines, even when it is observed in small scales of $g_{exc} \times I_0$. On the other hand, our results also indicate that the uncertainty about the synchronous and desynchronous states tends to be reduced as the coupled strength is increased (Fig. 11(c)).

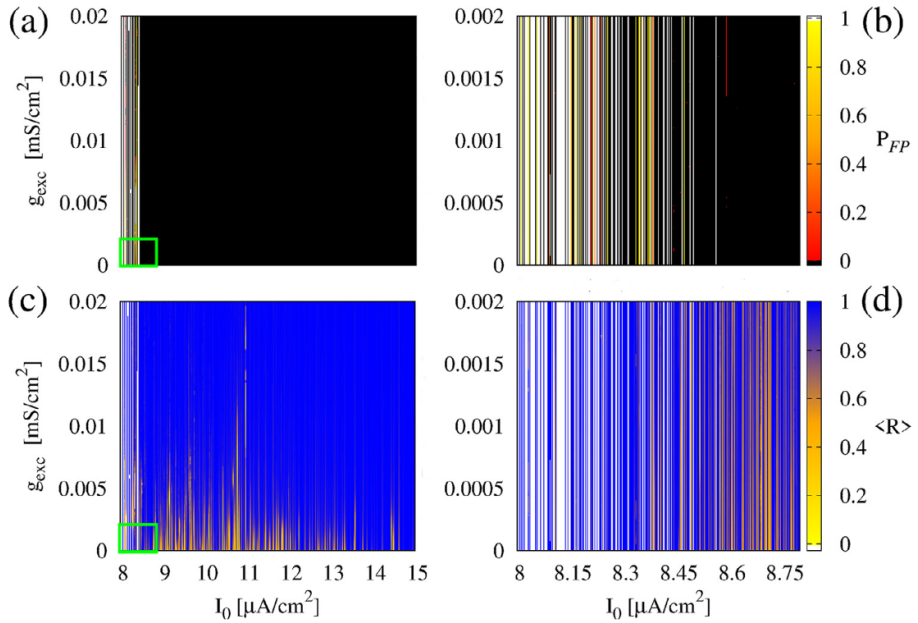

Fig. 11. Parameter space $g_{exc} \times I_0$ for coupled HH neurons under an external current randomly pulsed with $\Gamma = 0.35$ μA/cm^2. The panels (a) and (b) display P_{FP} in colour scale. The panels (c) and (d) show $\langle R \rangle$ in colour scale. The increasing of the coupling reduces the uncertainty in the synchronisation when random pulse is applied.

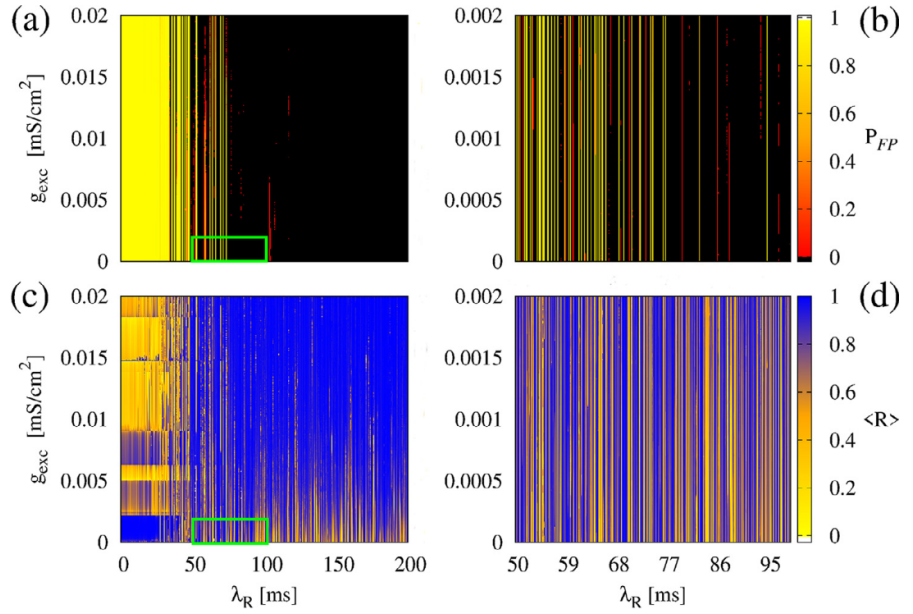

Fig. 12. Parameter space $g_{exc} \times \lambda_R$ for coupled HH neurons under an external current with mixed pulses considering $I_0 = 9$ μA/cm^2 and $\Gamma = 0.35$ μA/cm^2. The panels (a) and (b) display P_{FP} in colour scale. The panels (c) and (d) shows $\langle R \rangle$ in colour scale. When λ_R is larger than a certain value (~ 40 ms), an increasing of the coupling is able to reduce the uncertainty.

We analyse an external current composed by a sequence of periodic and random pulses with a Γ amplitude. As discussed in the uncoupled neurons, we focus on the changes in the neuronal activities due to the time windows λ_R of random pulses embedded in a sequence of periodic pulses. Firstly, we consider periodic pulses with $I_0 = 9.0$ μ A/cm^2, $\Gamma = 0.35$ μA/cm^2, $\Delta t = 1$ ms, $\lambda_P^0 = 200$ ms, and $\lambda_R = 0$ ms. As shown in Fig. 12(a) (magnification of the green box in Fig. 12(b)), the windows λ_R with sizes approximately superiors to 40 ms are enough to generate some changes in the network, mainly considering that after 40 ms, uncertainties associated with the fraction of the neurons spiking or in silence can be observed. With regard to the spike synchronisation, our results also indicate that after 40 ms, the uncertainty behaviour can also be identified in the parameter space $g_{exc} \times \lambda_R$, as shown in Fig. 12(c) and highlighted in Fig. 12(d).

In our simulations, we observe that the external pulse plays an important role in the dynamics of the network. However, a weak coupling can improve the appearance of neuronal synchronous behaviour. On the other hand, the bistability does not exhibit a significant change due to a weak coupling strength. Furthermore, the synaptic coupling can reduce the uncertainty in the neuronal synchronisation.

5. Conclusions

In this work, we study the effects of pulsed perturbations in the dynamics of coupled and uncoupled Hodgkin Huxley neurons. Our results show that depending on the external current with a constant amplitude, the uncoupled or coupled neurons can remain in silence, spike or between both activities (bistability). For the analysed set of initial conditions, the increase of the current amplitude can support spike synchronisation in the uncoupled or weakly coupled neurons.

Considering periodic pulses, we observe changes in the range of the parameters in which neurons spike or not and synchronisation occur. When pulses are randomly applied, we also identify changes in the range of the parameters related to the emergence of the neuronal spikes. Moreover, the random pulses may introduce an uncertainty about the ranges of the bistable states, as well as in the synchronous and desynchronous patterns.

Our numerical simulations indicate that small intervals of random pulses embedded in a sequence of periodic pulses can be enough to generate uncertainty not only in the neuronal activities, but also in the synchronous behaviour. As well known, synchronous patterns can be associated with neurological disorders (such as epilepsy) and the perturbations to sensory stimulus. This way, the understanding about the conditions and parameters range in which such activities emerge plays a crucial role in neuroscience. However, as we suggest along this work, depending on the type of perturbation, it may not be trivial the determination of the parameters range related to the onset of synchronisation.

In summary, by understanding the effects of external stimuli in the brain, we can better choose appropriate methods for the control and treatment of brain diseases. Experimental protocols considering different temporal patterns of electrical stimulations have presented a promising alternative for the treatment of epileptic seizures [33]. In this work, we consider external perturbations in a neuronal network according to different protocols of stimulations introduced in [33]. One of our main contribution is to show the appearance of uncertainties in the neuronal activities. The uncertainty behaviour can emerge due to the small windows of random pulsed inputs, leading the neuronal activities to an undesirable dynamics. In the context of experimental analyses, the noise in the stimulation can be one of the sources of uncertainty in the neuronal dynamics.

In future works, we plan to analyse the effect of changing the rewiring probability p of the coupled network on P_{FP} and $\langle R \rangle$. There are some studies that suggest that the brain is connected by means of a small-network architecture.

Credit author statement

All authors discussed the results and contributed to the final version of the manuscript.

Declaration of Competing Interest

I hereby certify that this research article consists of original, unpublished work which is not under consideration for publication elsewhere. There is no conflict of interest.

I hope your favorable consideration for publication.

Acknowledgments

The authors acknowledge the financial support from the São Paulo Research Foundation (FAPESP, Brazil) (Gr-ants Nos. 2015/50122-0, 2018/03211-6, 2019/09150-1 and 2020/04624-2). The National Council for Scientific and Technological Development (CNPq), the Coordenação de Aperfeiçoamento de Pessoal de Nível Superior - Brasil (CA PES) and the Fundação Araucária.

References

[1] Biju KS, Jibukumar MG. Classification of ictal EEG using modeling based spectral and temporal features on instantaneous amplitude-frequency components of IMFs. Biomed Eng: Appl Basis Commun 2018;30:1850042.
[2] Perrey S. Promoting motor function by exercising the brain. Brain Sci 2013;3:101–22.
[3] Gilbert CD, Sigman M. Brain states:top-down influences in sensory processing. Neuron 2007;54:677–96.
[4] Smith S. Technologies for imaging neural activity in large volumes. Nat Neurosci 2016;19:1154–64.
[5] Pereda AE. Electrical synapses and their functional interactions with chemical synapses. Nat Rev Neurosci 2014;15:250–63.
[6] Kreiman G, Koch C, Fried I. Imagery neurons in the human brain. Nature 2000;408:357–61.
[7] Kass RE, S-I A, Arai K, Brown EN, Diekman CO, Diesmann M, et al. Computational neuroscience: mathematical and statistical perspectives. Annu Rev Stat Appl 2018;5:183–214.
[8] Blundell I, Brette R, Cleland TA, Close TG, Coca D, Davison AP, et al. Code generation in computational neuroscience: areview of tools and techniques. Front Neuroinform 2018;12:68.
[9] Shilnikov A, Calabrese RL, Cymbalyuk G. Mechanism of bistability: tonic spiking and bursting in a neuron. Phys Rev E 2005;71:056214.
[10] Lapicque L. Recherches quantitatives sur l'excitation electrique des nerfs traitee comme une polarization. J Physiol Pathol Gen 1907;9:620–35.
[11] Abbott LF. Lapicque'S introduction of the integrate-and-fire model neuron. Brain Res Bull 1999;50:303–4.
[12] Hodgkin AL, Huxley AF. A quantitative description of membrane current and its application to conduction and excitation in nerve. J Physiol 1952;117:500–44.
[13] Bashkirtseva I, Ryashko L. Analysis of excitability for the fitzhugh–nagumo model via a stochastic sensitivity function technique. Phys Rev E 2011;83:061109.
[14] Morris C, Lecar H. Voltage oscillations in the barnacle giant muscle fiber. Biophys J 1981;35:193–213.
[15] Borges FS, Protachevicz PR, Lameu EL, Bonetti RC, arosz KC, Caldas IL, Baptista MS, Batista AM. Synchronised firing patterns in a random network of adaptive exponential integrate-and-fire neuron model. Neural Netw 2017;90:1–7.
[16] Masuda N, Aihara K. Global and local synchrony of coupled neurons in small–world networks. Biol Cybern 2004;90:302–9.
[17] CAS B, Lameu EL, Batista AM, Lopes SR, Pereira T, Zamora-López G, Kurths J, Viana RL. Phase synchronization of bursting neurons in clustered small-world networks. Phys Rev E 2012;86:016211.
[18] CAS B, Batista AM, de Pontes J, Viana RL, Lopes SR. Chaotic phase synchronization in scale-free networks of bursting neurons. Phys Rev E 2007;76:016218.
[19] CAS B, Lopes SR, Viana RL, Batista AM. Delayed feedback control of bursting synchronization in a scale-free neuronal network. Neural Netw 2010;23:114–24.
[20] Wang W, Chen G, Perc M. Synchronous bursts on scale-free neuronal networks with attractive and repulsive coupling. PLoS ONE 2011;6:e15851.
[21] Antonopoulos CG, Fokas AS, Bountis TC. Dynamical complexity in the c. elegans neural network. Eur Phys J Spec Top 2016;225:1255.
[22] Antonopoulos CG. Dynamic range in the c. elegans brain network. Chaos 2016;26:013102.
[23] Hizanidis J, Kouvaris NE, Zarmora-López G, Díaz-Guilera A, Antonopoulos CG. Chimera-like states in modular neural networks. Sci Rep 2016;6:19845.
[24] C-C H, GAPC B, O'Neill MA, Scannell JW, Young MP. Anatomical connectivity defines the organization of clusters of cortical areas in the macaque monkey and the cat. Phil Trans R Soc Lond B 2000;355:91–110.
[25] JCP C, FAS F, Reis AS, Iarosz KC, Caldas IL, Batista AM, Viana RL. Network properties of healthy and alzheimer brains. Physica A 2020;547:124475.
[26] Borges RR, Borges FS, Lameu EL, Batista AM, Iarosz KC, Caldas IL, Viana RL, MAF S. Effects of the spike timing-dependent plasticity on the synchronisation in a random hodgkin-huxley neuronal network. Commun Nonlinear Sci Numer Simulat 2016;34:12–22.
[27] Andreev AV, Frolov NS, Pisarchik AN, Hramov AE. Chimera state in complex networks of bistable hodgkin-huxley. Phys Rev E 2019;100:022224.
[28] CAS B, Viana RL, FAS F, Lopes SR, Batista AM, JCP C. Control of bursting synchronization in networkd of hodgkin-huxley-type neurons with chemical synapses. Phys Rev E 2013;87:042713.
[29] Khoshkhou M, Montakhab A. Explosive, continuous and frustrated synchronization in spiking hodgkin-huxley neural networks: the role of topology and synaptic interaction. Physica D 2020;405:132399.
[30] Wang Y, DTW C, Wang ZD. Coherence resonance and noise-induced synchronization in globally coupled hodgkin-huxley neurons. Phys Rev E 2000;61:740.
[31] Nakamura O, Tateno K. Random pulse induced synchronization and resonance in uncoupled non-identical neuron models. Cogn Neurodyn 2019;13:303–12.
[32] Protachevicz PR, Borges FS, Lameu E, Ji P, Iarosz KC, Kihara AH, Caldas IL, Szezech JD, Baptista MS, EEN M, Antonopoulos CG, Batista AM, Kurths J. Bistable firing pattern in a neural network model. Front Comput Neurosci 2019;13:1–19.

[33] Cota VR, de Oliveira JC, LCM D, MFD M. Nonperiodic stimulation for the treatment of refractory epilepsy: applications, mechanisms, and novel insights. Epilepsy Behav 2021;121:106609.
[34] Golomb D, Rinzel J. Dynamics of globally coupled inhibitory neurons with heterogeneity. Phys Rev E 1993;48:4810.
[35] Destexhe A, Mainen ZF, Sejnowki TJ. An efficient method for computing synaptic conductances based on a kinetic model of receptor binding. Neural Comput 1994;6:14–18.
[36] Noback CR, Strominger NL, Demarest RJ, Ruggiero DA. The human nervous system:. Structure and Function (sixth ed.). Totowa, NJ: Humana Press; 2005.
[37] Borges RR, Borges FS, Lameu EL, Batista AM, Iaros KC, Caldas IL, Antonopoulos CG, Baptista MS. Spike timing-dependent plasticity induces non-trivial topology in the brain. Neural Netw 2017;88:58–64.
[38] Popovych OV, Yanchuk S, Tass PA. Self-organized noise resistance of oscillatory neural networks with spike timing-depen-dent plasticity. Sci Rep 2013;3:2926.
[39] Keener J, Sneyd J. Mathematical physiology. New York: Sprin-ger; 1998.
[40] Acebrón JA, Bonilla LL, CJP V, Ritort F, Spigler R. The kuramoto model: a simple paradigm for synchronization phenomena. Rev Mod Phys 2005;77:137.
[41] Chatterjee M, Robert ME. Noise enhances modulation sensitivy in cochlear implant listeners: stochastic resonance in a prosthetic sensory system? JARO 2001;02:159–71.